

MANEUVERABILITY OF AN UAV WITH COANDA EFFECT BASED LIFT PRODUCTION

Nikola Mirkov*, Bosko Rasuo**

*PhD student, University of Belgrade, Institute of Nuclear Sciences 'Vinca', **University of Belgrade, Faculty of Mechanical Engineering
 nikolamirkov@yahoo.com; brasuo@mas.bg.ac.rs

Keywords: Coanda Effect, Unmanned Aerial Vehicle, Computational Fluid Dynamics, 6-DOF model

Abstract

This paper presents a study built around numerical simulations of axially-symmetric body representing an Unmanned Aerial Vehicle (UAV) that uses Coanda effect for producing lift force. The purpose is to make a maneuverability study of such an UAV under flow conditions denoted as asymmetric Coanda effect. Dynamically changing the flow picture enables change of net force on the aircraft. Capability to control the direction of the net force is used for maneuvering the aircraft. All simulations are done using Finite-volume computational fluid dynamics (CFD) code. Turbulence is accounted using $k - \omega$ Shear Stress Transport model. The study presents natural continuation of research efforts reported in [1].

1 Introduction

There is a renewed interest in recent times in use of the Coanda effect for vertical/short take-off and landing (V/STOL) aircraft as it cuts the need for long runways and reduces the time to achieve useful fight. This is particularly true for UAV's, where less expensive prototypes encourage experimenting with novel concepts. Attention to Coanda effect has additionally been drawn by recent (2010) centenary of it's discovery. Our approach relies on CFD as a tool for fast and efficient case study under variation of multiple parameters. This approach enables greater flexibil-

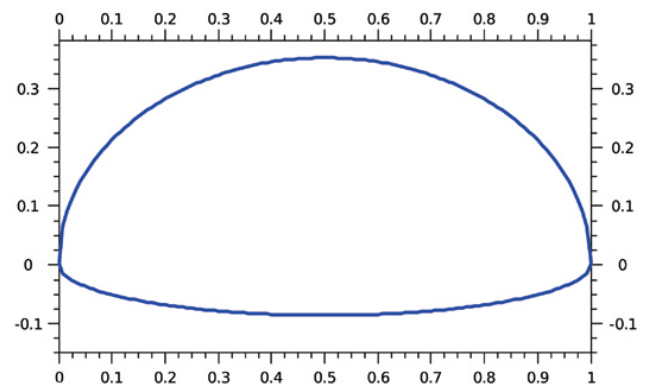


Fig. 1 Cross section of the Coanda effect UAV

ity in evaluating many different aircraft geometries and flow configurations hardly accessible with real models. Also coupling with optimisation algorithms is available, that could generate optimized UAV shapes.

In our previous paper [1] we have showed a universal parametric geometry representation of such UAV, based on Bernstein polynomials (Fig. 2). By universal it is meant that such a representation spans a complete design space. Such representation is amenable to shape optimization study. An optimized shape is still an open question and calls for future study and in a meanwhile an arbitrary representative of the design space is chosen for this study (Fig. 1).

The description of lift force generation on this class of UAV is following.

Flow from the inlet located at the top of the UAV is being immediately attached to the upper surface due to Coanda effect (see Fig. 3). The

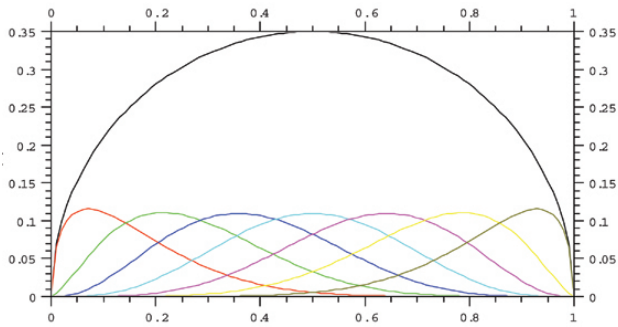


Fig. 2 Decomposition of the upper arc using 6th order Bernstein polynomials

air jet stays attached along complete extent of the upper surface, entraining the increasing amount of air. Surrounding air entrainment and increase in wall-jet velocity as it approaches the upper surface edge, produces decrease of pressure and upward suction force. At the same time pressure increase is sensed at the bottom surface.

It has been shown, that changing the flow picture on Coanda effect UAV is responsible for changing the force exerted on the body. Increase in the upward force is correlated to the strength and size of vortex below the body. Varying the parameters of Coanda effect produces different forces and can be used for maneuvering the UAV.

In this paper we will describe a framework for such study, consisting of fluid dynamics solver coupled to unconstrained rigid-body motion solver. Results of aerodynamic study is also presented with an emphasis on requirements for controllable complex motion of the UAV.

2 Simulation algorithms

2.1 Flow solver - a visit to coffee shop

In our study we use an in-house code *Cappuccino - a CAFFA with some FOAM*. It is cell-centered second order accurate finite volume code, intended for block-structured non-orthogonal geometries, with collocated variable arrangement. It originated from the well know CAFFA code [2] after extensive development. Features that were added include a number of high order bounded schemes for convective fluxes (GAMMA scheme is used in this study), least-square gradient re-

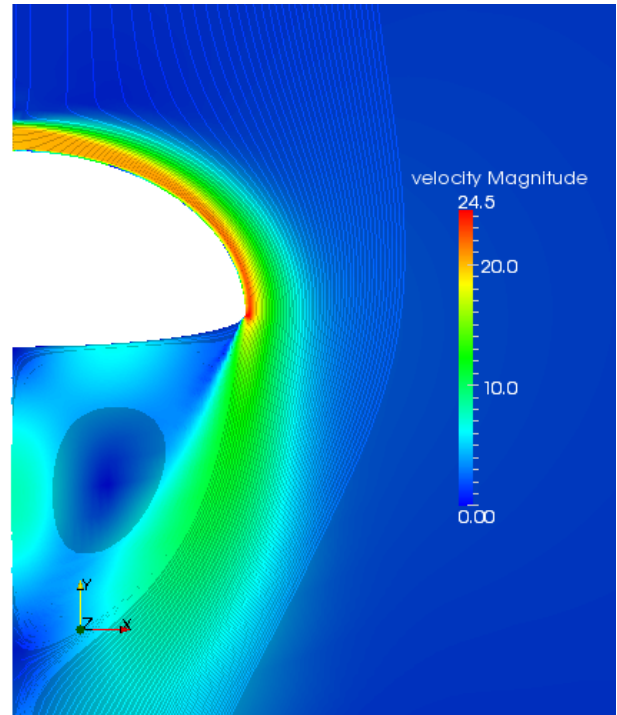


Fig. 3 Symmetric Coanda effect - flow picture, only one half is shown

construction (overdetermined system solved using QR decomposition based on Householder reflections). Geometric multigrid is used to speed-up outer (SIMPLE) iterations, with SIP solver as a smoother.

Special attention is given to turbulence models where wide range of applications is anticipated. Among implemented models most prominent are Menter's $k - \omega$ Shear Stress Transport [3] [4] (used in this study) and EARSM of Wallin and Johansson [5]. Automatic wall boundary condition approach [6] is used, which is particularly suited when, during geometric multigrid procedure, a wall-coarsening takes place which requires a paradigm shift in treating the cells in the first layer next to the wall.

2.2 Aerodynamic forces and moments

The aerodynamic forces acting on a body immersed in a fluid are calculated in usual way, pressure and viscous friction forces are integrated over the body to give the net forces. As a consequence of discrete representation of the body's

surface, integrations are replaced by summations of forces over elementary surfaces. Other than aerodynamic forces, we also take into account the force of gravity, and the interplay of this body force and surface aerodynamic forces gives rise to complex three-dimensional motion.

The procedure may be summarized in the following way.

At each time step, after flow field calculation, we find pressure and viscous drag forces acting on elementary surfaces of discrete representation of body's surface (see Fig. 6). Summing the forces over surface mesh elements we get net forces acting on a body.

Knowing the radius vector from the center of mass (c.m.) to every element of the body's surface mesh, as well as pressure and viscous friction force vectors acting on these elements we are able to reconstruct moments. Summing the moments over surface mesh elements we get net moments acting on the body.

Forces and moments are further fed into the rigid-body solver, which integrates Newton-Euler equations and updates position and orientation of the UAV with respect to the Earth coordinate system (Fig. 4). Repeatedly calling the rigid-body integrator we reconstruct trajectory and orientation as a function of time.

2.3 Rigid-body Integrator

Complex three-dimensional motion of the body is broken into translational motion of the center of mass in inertial coordinate system, and rotation expressed in coordinate system attached to the body. Newton-Euler system of equations is used as a model of such unconstrained motion of a rigid body, commonly known as Six-degree-of-freedom (6-DOF) motion.

We may choose two approaches of coupling the fluid flow simulation with rigid-body motion integrator. First approach is to couple the 6-DOF solver with fluid solver at each time-step, the other, more economic one, is by computing UAV's trajectory based on a database collected during nonstationary CFD simulation with a particular flight control scenario. Database consists

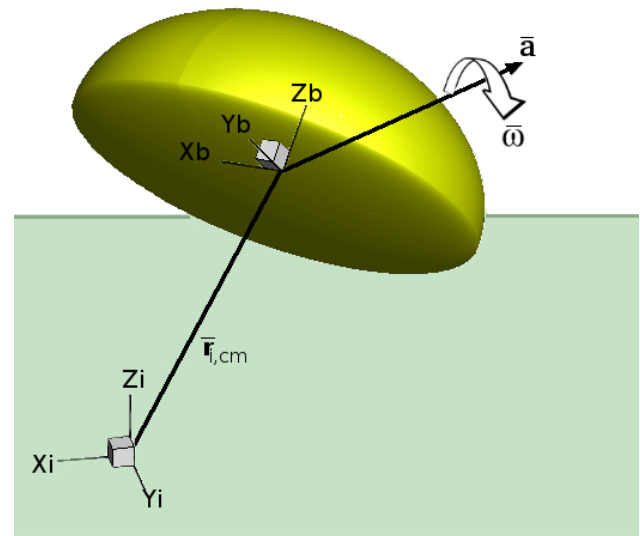


Fig. 4 Two coordinate systems used to express the unconstrained motion of a rigid body

of force and moment data, as well as the principal moments of inertia, which remain constant during the simulation. In our study no relative motion is needed to be taken into account, therefore single mesh is used.

Our rigid-body solver includes interface to DOPRI5, an implementation of the explicit fourth order Runge-Kutta method with fifth order correction by Dormand and Prince [7] [8]. In two successive integrations it provides angular momentums and Euler parameters (quaternions). Transformation matrix is obtained from Euler parameters, and is used to reposition the body in the inertial coordinate system.

Implementation of the rigid-body solver used in this study is based on solver found in [9]. For further details readers are urged to consult this reference. The main difference between the two solvers is in Runge-Kutta algorithm. During solver validation studies we found that DOPRI5 provides more accurate integration compared to common fourth-order Runge-Kutta integrator.

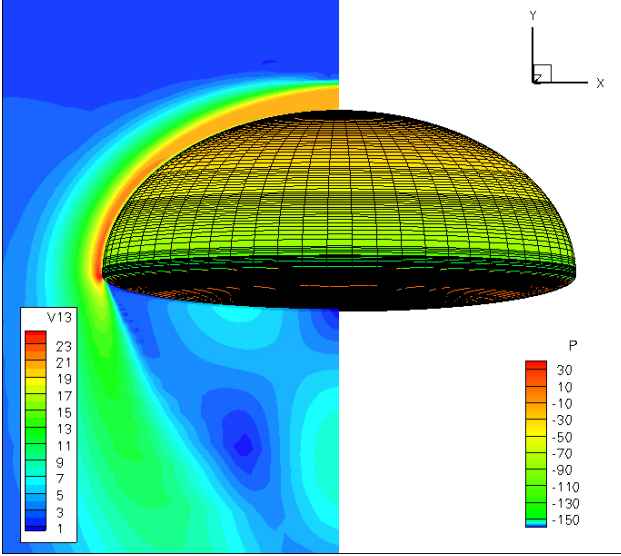


Fig. 5 Pressure on the body surface

3 Simulation details

Case that we have studied has moderately small Reynolds number, $Re = 63775$ based on mean velocity and inlet height. Velocity is uniform across the inlet ($U_b = 20$ m/s). Mesh consists of roughly 500 000 cells. We haven't considered any particular method in which the inlet flow is generated. We have to remind however, that in such case some additional information should be provided, such as swirl velocity component, if a fan is used for providing inflowing air.

To generate lateral forces which would produce forward motion we experimented with varying inlet velocity along the circumference of the inlet, resulting in an asymmetric Coanda effect.

4 Results-flow picture

For the given configuration and inlet conditions, air jet is able to stay attached on upper surface, and the presence of Coanda effect is clearly visible (see Fig 5). We are able to observe entrainment of the surrounding air into the jet which causes gradual increase of air jet velocity as the jet is approaching the upper's surface edge. At the edge point, velocity has an 25% increase compared to the inlet and reaches 25 m/s.

This is followed by pressure decreasing on

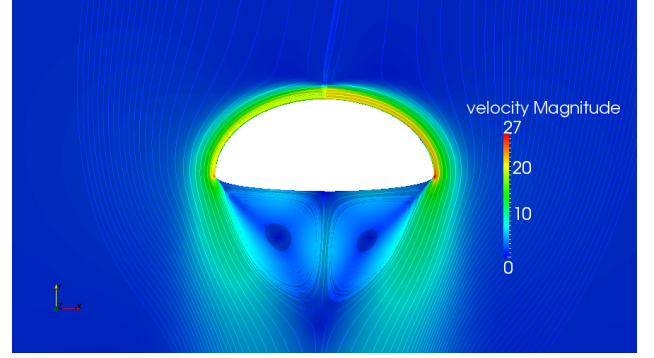


Fig. 6 Asymmetric Coanda effect - velocity magnitude and streamlines

the upper surface. Suction force is present, and is gradually increasing towards the edge of the upper surface. This produces upward net force, which is able to keep the UAV with described geometry and flow conditions in hovering flight even with the mass around 1.5 kg.

Varying the inlet velocity around the circumference produced asymmetric flow picture (cross section shown in Fig. 6). Asymmetry is most clearly visible by observing streamline pattern. Less surrounding air is entrained, velocity at the upper surface edge reaches smaller value. Pressure is unevenly distributed along the upper surface and lateral force is present which enables forward motion.

Due to strong curvature at the edge of the upper surface, wall jet flow is unable to stay attached. Separated flow patterns can be visualized with different techniques most frequently seen in the case of separated bluff body flows. One that we chose is by extracting time-averaged and instantaneous isosurfaces of the second invariant of velocity gradient tensor, defined in time-averaged case by following expression:

$$Q = -\frac{1}{2} \frac{\partial \bar{u}_i}{\partial x_j} \frac{\partial \bar{u}_j}{\partial x_i} = -\frac{1}{2} (\bar{S}_{ij} \bar{S}_{ij} - \bar{\Omega}_{ij} \bar{\Omega}_{ij}) \quad (1)$$

where S_{ij} and Ω_{ij} denote symmetric and anti-symmetric part of velocity gradient tensor respectively, and over-bar represents time-average (Fig. 7 and 8).

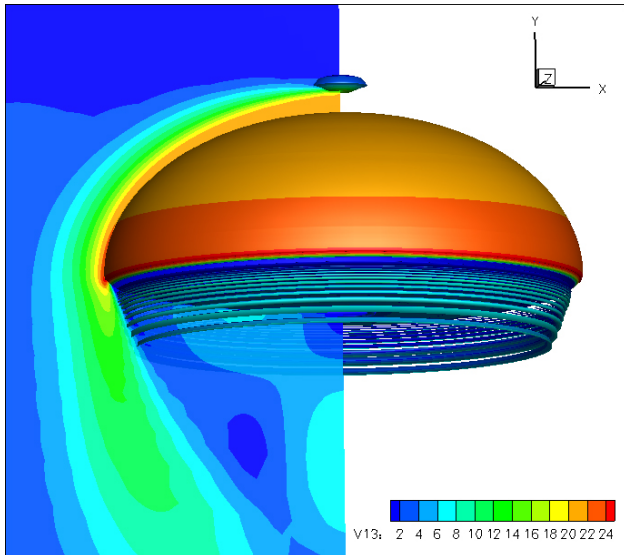


Fig. 7 Iso-surface of Q coloured by velocity magnitude

5 Conclusion

Using numerical simulation as a tool of choice we tackle the fascinating and in our opinion not fully exploited phenomena of Coanda effect based lift production. In this and in companion paper [1] we have set the framework for the exploration of multi-dimensional design space of Coanda effect UAV's. We propose procedures for different shape choices, lift force variation by flow control, maneuvering by thrust vectoring via wall jet control and asymmetric Coanda effect. Future studies will present results from non-stationary simulation with realization of complex three-dimensional motion. We hope our preliminary results will encourage researchers to dedicate their attention to these types of UAV's, unleashing the imagination while conquering the airspace.

References

- [1] Mirkov, N., Rasuo, B., *Numerical simulation of air jet attachment to convex walls and applications*, Proceedings of 27th International Congress of the Aeronautical Sciences - ICAS 2010, Nice, France 2010.
- [2] Ferziger, J.H., Peric, M., *Computational Methods for Fluid Dynamics*, 2nd edition, Springer, 1999.

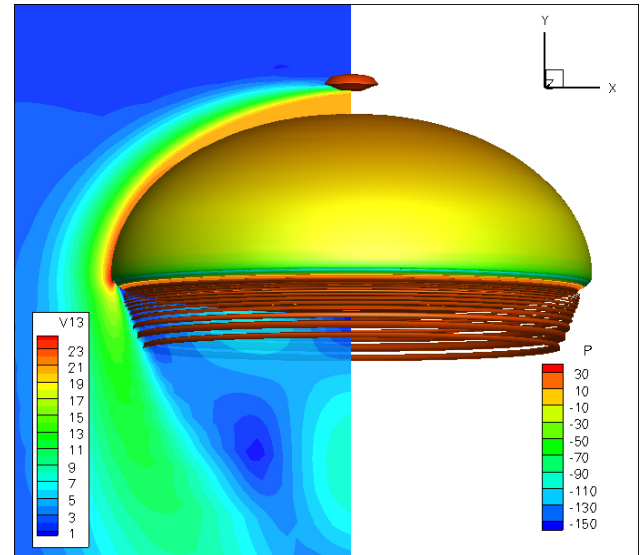


Fig. 8 Iso-surface of Q coloured by pressure

- [3] Menter, F. R., "Two-Equation Eddy-Viscosity Turbulence Models for Engineering Applications," *AIAA Journal*, Vol. 32, No. 8, pp. 1598-1605, August 1994.
- [4] Menter, F. R., Kuntz, M., and Langtry, R., *Ten Years of Industrial Experience with the SST Turbulence Model*, Turbulence, Heat and Mass Transfer 4, ed: K. Hanjalic, Y. Nagano, and M. Tummers, Begell House, Inc., pp. 625 - 632, 2003.
- [5] Wallin, S. and Johansson A., *A complete explicit algebraic Reynolds stress model for incompressible and compressible flows*, *Journal of Fluid Mechanics*, 403, pp. 89-132, 2000.
- [6] Menter, F., et. al., *The SST Turbulence Model with Improved Wall Treatment for Heat Transfer Predictions in Gas Turbines*, Proceedings of the International Gas Turbine Congress, Tokyo, November 2-7, 2003.
- [7] Dormand, J. R., Prince, P. J., *A family of embedded Runge-Kutta formulae*, *Journal of Computational and Applied Mathematics* 6 (1), pp. 19-26, 1980.
- [8] Hairer, E., Nørsett, S. P., Wanner, G., *Solving ordinary differential equations I: Nonstiff problems*, Berlin, New York: Springer-Verlag, 2008.
- [9] Murman, S.M., Aftosmis, M.J., Berger, M.J., *Simulation of 6-DOF Motion with a Cartesian Method*, AIAA-Paper 2003-1246, 2003.

Acknowledgement

The authors wish to express gratitude for the financial support of their research by Serbian Ministry of Science, through projects No. TR-33036 and TR-35006 respectively.

Copyright Statement

The authors confirm that they, and/or their company or organization, hold copyright on all of the original material included in this paper. The authors also confirm that they have obtained permission, from the copyright holder of any third party material included in this paper, to publish it as part of their paper. The authors confirm that they give permission, or have obtained permission from the copyright holder of this paper, for the publication and distribution of this paper as part of the ICAS2012 proceedings or as individual off-prints from the proceedings.